Materials Science and Engineering, A128 (1990) 77–89

Young's Modulus and Damping of Ti–6Al–4V Alloy as a Function of Heat Treatment and Oxygen Concentration

Y. T. LEE* and G. WELSCH

Department of Materials Science and Technology, Case Institute of Technology, Case Western Reserve University, Cleveland, OH 44106 (U.S.A.)

(Received September 8, 1989; in revised form January 10, 1990)

Abstract

Young's modulus and damping of texture-free Ti–6Al–4V alloy were evaluated at room temperature by longitudinal resonance vibration tests on cylindrical bars of measured length and density. Damping was determined from the half-width Δf of the resonance peaks. The alloy's properties were evaluated as a function of solution heat treatments between 600 and 1200 °C with subsequent quenching, aging treatments between 200 and 550 °C, and plastic deformation of solution-treated and quenched alloy. The effects of oxygen concentration were determined on identically produced Ti–6Al–4V alloys but with systematic variation of oxygen concentration between 0.17 and 0.30 wt.% (0.50–0.88 at.%). Heat treatment alone accounts for variations in Young's modulus E_0 by as much as 10% of the nominal value and in damping by more than an order of magnitude. Interstitial oxygen increases Young's modulus in addition to and independent of heat treatment, according to

$$E_{alloy}\ (GPa) = E_0 + 13.5\ (\text{weight per cent of oxygen})$$

Oxygen was found to have little effect on the damping capacity at room temperature.

Low Young's modulus values are obtained when the second phase contains a vanadium enrichment of about 10 wt.% V. In the quenched state the second phase is actually a metastable ($\beta + \alpha''$) phase mixture with a very low specific modulus value of about 74 GPa and a high specific damping capacity of 1×10^{-2}. The largest damping capacity ($Q^{-1} > 10^{-3}$) of the alloy is obtained after solution treatment and quenching (STQ) from 800 °C. High damping is also obtained after STQ from just below 1000 °C. The high damping is believed to arise from anelastic deformation of the second phase when it is present as metastable (β–α'') or (α''–α') mixtures respectively. The damping capacity of STQ-treated alloys decreases rapidly on aging, even at low aging temperatures of 200 °C, to Q^{-1} values of less than 1×10^{-4}.

1. Introduction

Young's modulus is an important property for engineering design. Titanium alloys have a relatively low modulus compared with other high strength engineering materials [1]. While Young's modulus of most materials can be taken as constant, *i.e.* heat treatments and compositional variations have negligible effects, the Ti–6Al–4V alloy behaves differently in this respect. Heat treatment has a large effect on the modulus. Significant variations also occur with texture because of strong crystallographic anisotropy of the elastic constants of α-Ti [2, 3]. Several researchers have measured Young's modulus of α-Ti single crystals [4] as a function of alloy element concentration [5] and interstitial solute content [6, 7]. In general, it has been found that interstitial and substitutional α-stabilizing solutes increase the modulus, whereas β-stabilizing solutes decrease the modulus [7].

In a multiphase alloy the value of Young's modulus is determined by the specific moduli of the phases and by their volume fractions. In the Ti–6Al–4V alloy the volume fractions and compositions of the constituent phases depend on prior thermal–mechanical treatments and, as a consequence, Young's modulus depends not only on texture but on heat treatment as well. The published literature lists Young's modulus values of the Ti–6Al–4V alloy from 100 to 130 GPa [8–15]. Several references describe effects of heat

*Present address: DLR (German Aerospace Research Establishment), Institut für Werkstoff-Forschung, Postfach 906058, 5000 Köln 90, F.R.G.

0921-5093/90/$3.50

treatment, but the separation from texture effects is often not clear. The texture dependency in α-Ti was systematically investigated by Larsen and Zarkades [2], who showed a variation of Young's modulus from 100 GPa perpendicular to the C axis to 145 GPa parallel to the C axis. Similar anisotropy of Young's modulus was found for the Ti–6Al–4V alloy [2, 3] with values ranging from 100 to 133 GPa. The effects of heat treatment were not reported in their work. A genuine average value of Young's modulus can only be measured on a texture-free polycrystalline alloy, for example, on an alloy prepared by sinter compaction of randomly oriented powder particles to full density.

Young's modulus and damping are sensitive indicators of phase changes and structural changes within the phases, and can be used for their interpretation. Damping is the more complex mechanical property of the two, because it may depend on several mechanisms of energy dissipation. However, damping peaks are often correlatable to modulus changes as a function of temperature or phase changes. Its engineering significance is due to the ability to reduce vibration and sound transmission in structural parts by dissipation of elastic strain energy during each strain cycle [16]. A number of articles have been published on damping of titanium alloys as a function of heat treatment, alloy content, temperature, and frequency [17–25]. The damping coefficient of mill-annealed Ti–6Al–4V alloy is generally of low value ($Q^{-1} < 10^{-4}$) [13]. Higher damping values at room temperature have been interpreted to be due to the presence of metastable β or α'' martensite phase [17, 19, 20]. Damping peaks have been detected at several temperatures and have been interpreted to be due to dislocation breakaway from point defects (peak at $-160\,^{\circ}C$), and due to rearrangement of interstitial oxygen atoms (peak at $325\,^{\circ}C$). Damping can be increased by the addition of β-isomorphous elements, such as molybdenum, vanadium and tantalum, and is decreased by aging treatments [21]. While titanium alloys with stable $\alpha+\beta$ phase mixtures have low damping capacity ($Q^{-1} < 10^{-4}$), an order of magnitude increase can be achieved by certain heat treatments and quenching.

The heat treatments include solution treatments and aging treatments. They cause variations in the volume fractions of α and β phases. A further variable is that the second phase may be present as vanadium-stabilized β phase (after slow cooling or aging) or as metastable β phase or as α''-martensite or as an α'-martensite (after quenching).

Oxygen, being a strong α stabilizer, influences the relative stability of the phases and affects their volume fractions [26, 27]. Oxygen atoms may also have a direct influence on modulus and damping capacity through effects on the interatomic bond strength.

The objectives of the present work are as follows: (1) determination of the dependence of Young's modulus on heat treatment in texture-free alloy; (2) determination of the effect of oxygen concentration on Young's modulus; (3) determination of the effects of heat treatment and oxygen concentration on room temperature damping capacity in longitudinal resonance vibrations.

2. Material and experiments

2.1. Material

Specimens of the Ti–6Al–4V alloy were made by powder metallurgy processing with 0.17, 0.24, and 0.30 wt.% O (0.50, 0.70, and 0.88 at.%). Elemental powder compacts were sintered at $1260\,^{\circ}C$ to over 99% of theoretical density. The density was measured according to ASTM method B328-73 [28]. The measured density was taken into account in the modulus evaluation. The chemical composition of each specimen was determined by spectrographic analysis. The compositions are given in Table 1. The alloy's microstructure is shown in Fig. 1. It has a nearly equiaxed grain structure and is free of texture, a prerequisite for mechanical isotropy and the evaluation of the isotropic Young's modulus.

TABLE 1 Chemical compositions of sintered compacts in weight per cent

Ti	*Al*	*V*	*Fe*	*Na*	*Cl*	*O*	*N*	*C*
Balance	6.2	4.1	0.18	0.10	0.12	0.17 (0.50 at.%)	0.02	0.02
Balance	6.1	4.1	0.03	0.10	0.10	0.24 (0.75 at.%)	0.01	0.02
Balance	6.1	4.1	0.08	0.10	0.10	0.30 (0.88 at.%)	0.01	0.02

A quantitative description of the alloy's microstructure has been previously published [29, 30].

Specimens were solution heat treated at temperatures between 600 and 1200 °C for 1 h each and then water quenched. In this way, several phase volume ratios and phase compositions were obtained. Much of the interest was focused on the 800 °C solution-treated and quenched (STQ) condition which results in 10–20 vol.% of highly metastable β phase, the balance being α phase, and which imparts mechanical softness to the alloy [15]. The 800 °C STQ condition serves as a starting point for many of the aging heat treatments and for strain-induced transformation experiments. Aging heat treatments were carried out at 200, 350 and 550 °C for up to 100 h on specimens that had been quenched from various solution treatment temperatures. The microstructures developed during the aging treatments consisted of α phase and vanadium-enriched β phase. Depending on the oxygen concentration and aging temperature, the α phase may contain a very small volume fraction of fine Ti_3Al precipitates, while the β phase may contain precipitates of α or ω phase [27].

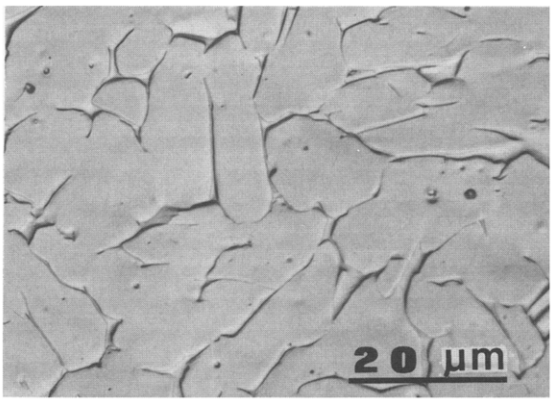

Fig. 1. Optical micrograph of an etched cross-section of a sinter-compacted and furnace-cooled Ti-6Al-4V alloy. The microstructure consists mostly of α phase and of about 10 vol.% β phase. The alloy is near theoretical density (about 99.5%). Residual pores are visible. They are enlarged from the etching.

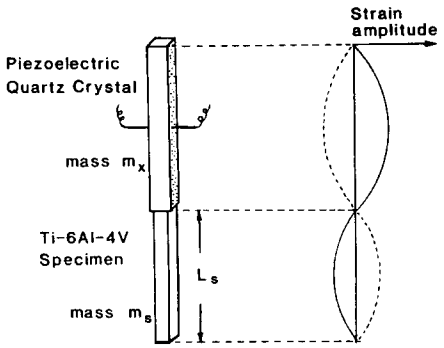

Fig. 2. Composite of specimen and quartz driving crystal used for the evaluation of Young's modulus and damping capacity in resonance vibration. The lengths of specimen and quartz crystal are matched so that the vibration nodes are at the free ends and at the bond interface.

2.2. *Microscopy*

Optical microscopy, scanning electron microscopy (SEM) and transmission electron microscopy (TEM) were used for the investigation of microstructures. TEM foils were prepared from the variously heat-treated specimens. Twin jet polishing was used for the preparation of TEM foils.

2.3. *Specimen geometries and deformation*

Rectangular bar specimens with a cross-section of 4 mm × 4 mm and 42 mm length were used to determine Young's modulus and damping by the resonance vibration method. To evaluate the effect of plastic deformation on Young's modulus and damping, some specimens were deformed at room temperature either by tension or by rolling. For the tensile deformation specimens with enlarged gripping ends were used. The uniformly deformed gauge sections were cut out and used for the resonance vibration measurements. The compressive deformation was performed by cold rolling the rectangular bars parallel to their long axis. The compressive strain was therefore in the thickness direction. Care was taken during rolling to avoid bending.

2.4. *Young's modulus measurement*

The evaluation of Young's modulus from tensile stress–strain curves is not very accurate. The accuracy of the elastic portion of stress–strain curves is further impaired by the superposition of quenched-in residual stresses on the nominal applied tensile stress. This complication is avoided when measuring in resonance vibration [31] at very small strain amplitudes ($\Delta\varepsilon \lesssim 10^{-5}$). Longitudinal vibration experiments were made with a composite of piezoelectrical quartz crystal (x) and specimen (s), as shown in Fig. 2. The lengths of initially oversized specimens were adjusted by grinding until their resonance frequency matched the resonance frequency f_x of the driving quartz crystal within 0.5%. The precise value of a specimen's resonance frequency was found from measurement of the composite's resonance frequency f_c, which is a

mass-weighted average of the quartz crystal's and the specimen's resonance frequencies [32, 33]:

$$f_s = \frac{f_c(m_x + m_s) - f_x m_x}{m_s} \quad (1)$$

f_s and m_s are the resonance frequency and the mass of the specimen, and f_x and m_x are the resonance frequency and the mass of the quartz crystal respectively. In the experiments f_x was 66 kHz. The mass of the composite is $m_x + m_s$. Young's modulus of the specimen is then obtained from

$$E = 4\rho L_s^2 f_s^2 \quad (2)$$

where ρ is the specimen density and L_s is the specimen length. The experimental accuracy was limited by the precision of the density and length measurements. The accuracy of the Young's modulus data was approximately ± 0.5 GPa which corresponds to $\pm 0.4\%$ of its absolute value.

2.5. *Damping measurement*

Damping causes broadening in the frequency resonance peak. The broadening is measured from the half-width Δf_s of the specimen's resonance peak that is obtained by plotting strain amplitude (or voltage output) *vs.* a variable driving frequency. The half-width Δf_s is a mass-weighted value, in analogy to eqn. (1), and is defined as the difference between the frequencies above and below the resonant peak at which the amplitude drops to $1/2^{1/2}$ of the peak value, *i.e.* a drop by 3 db. The damping coefficient Q^{-1} is given by

$$Q^{-1} = \frac{\Delta f_s}{f_s} \quad (3)$$

Q^{-1} is related to the logarithmic decrement δ of a freely decaying vibration through

$$\delta = \pi Q^{-1} \quad (4)$$

The accuracy of the measured damping coefficient was limited by the background damping, *i.e.* the damping of the quartz crystal and the damping caused by the air environment. Separate tests with the driving crystal alone showed that this background damping was of the order of 10^{-5}, which is small compared with the damping values of the quartz–specimen composites. Therefore, reasonable accuracy for the specimen's damping capacity Q^{-1} was obtained from the mass-weighted relation

$$Q^{-1} = \frac{Q_c^{-1}(m_x + m_s) - Q_x^{-1} m_x}{m_s} \quad (5)$$

where Q_c^{-1} and Q_x^{-1} are the specific damping coefficients of the composite and the quartz crystal respectively.

3. Results and discussion

3.1. *Volume fractions of phases*

The temperature dependence of the volume fractions of α and β phases is plotted in Fig. 3 for alloys with various oxygen concentrations. The curves reflect the α-stabilizing effects of oxygen, causing the transus temperature to rise [26] by

$$T_{\text{transus}}\,(^\circ\text{C}) = 937 + 243\,[\text{O}] \quad (6)$$

where [O] is in weight per cent.

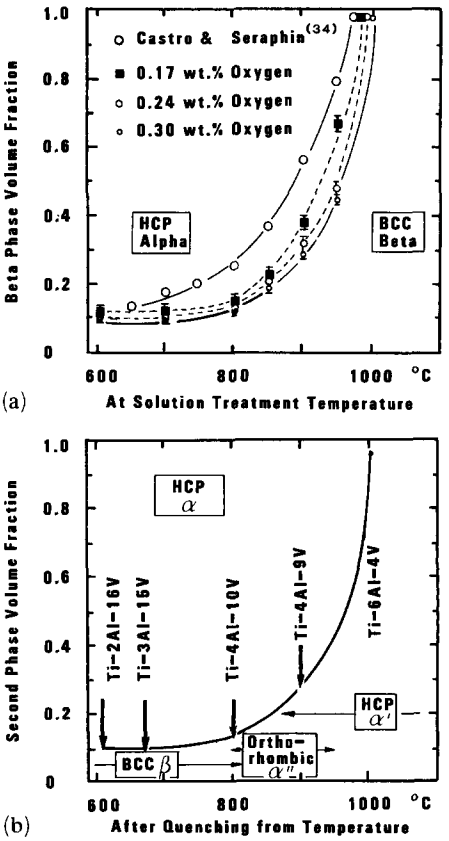

Fig. 3. (a) Equilibrium phase volume fraction of α and β phases as a function of solution treatment temperature. Oxygen increases the transus temperature and decreases the volume fraction of β phase below the transus. (b) After STQ, the second phase has different chemical compositions and crystal structures, *i.e.* h.c.p. α' phase, or orthorhombic α'' phase or b.c.c. β phase.

The composition of the hexagonal α phase varies little over the heat treatment temperature range [30, 34] and its mechanical properties are also little affected by heat treatment [27]. There are large compositional variations in the β phase, however. Localized enrichment of the β phase with vanadium occurs in proportion to the reduction in the volume fraction of β phase [34]. When β phase is vanadium enriched to about 15 wt.%, it retains the b.c.c. crystal structure on quenching to room temperature, *i.e.* it is stabilized, whereas vanadium-lean β compositions transform martensitically into α'' or α' phases on quenching. Of particular interest is the quenched structure of β phase with about 10 wt.% V. It is a highly metastable b.c.c. structure which is on the verge of transforming into orthorhombic α'' martensite. In this condition it is mechanically soft, and stress-induced phase transformation to α'' can readily occur. Also, its elastic modulus is low in this condition. The mechanically softest two-phase Ti-6Al-4V alloy is obtained after quenching from around 800 °C, even though the volume fraction of metastable β-α'' phase is only 0.10–0.20. The optimum solution treatment and quenching temperature for obtaining the softest condition of the alloy depends on oxygen concentration. According to Kahveci and Welsch [26] this dependence is similar to that of the transus temperature:

$$STQ_{softest}\,(°C) = 797 + 163\,[O] \qquad (7)$$

where [O] is in weight per cent and $STQ_{softest}$ is the STQ temperature for which the lowest alloy strength and the lowest Young's modulus are obtained.

3.2. *Microstructures*

3.2.1. *Microstructures after solution treatment and quenching*

Three microstructures are shown in Fig. 4. They were obtained after quenching from 1200 °C (Fig. 4(a)), after quenching from near the transus temperature of 1000 °C (Fig. 4(b)), and after quenching from 800 °C (Fig. 4(c)). After quenching from above the transus temperature, *e.g.* 1200 °C, the microstructure is that of α'-martensite. The martensite laths are coarser the higher the STQ temperature is. The 800 °C STQ microstructure (Fig. 4(c)) is a mixture of α phase plus β-α'' as the second phase. By microhardness indentation measurements it has been shown that the layers of β-α'' phase (light phase in Fig. 4(c)) are the mechanically soft regions [35]. The internal structure of the β phase and of its derivatives, the α'' or α' phases, are most important for Young's modulus and damping. The morphology of the phase aggregates, *i.e.* whether it is lamellar or equiaxed, is of relegated importance here. Apart from texture effects, the effect of phase morphology on Young's modulus and damping is considered small relative to the effects of crystal structure, in particular the effects of instability of the β phase and its derivative martensite phases. Phase morphology can be modified by thermal-mechanical treatment and is of importance for strength, fracture and fatigue properties [36].

3.2.2. *Microstructure of metastable β phase after pre-straining*

The transformation of metastable β phase to the orthorhombic α'' phase can be aided by applied stress. The more severe the metastability,

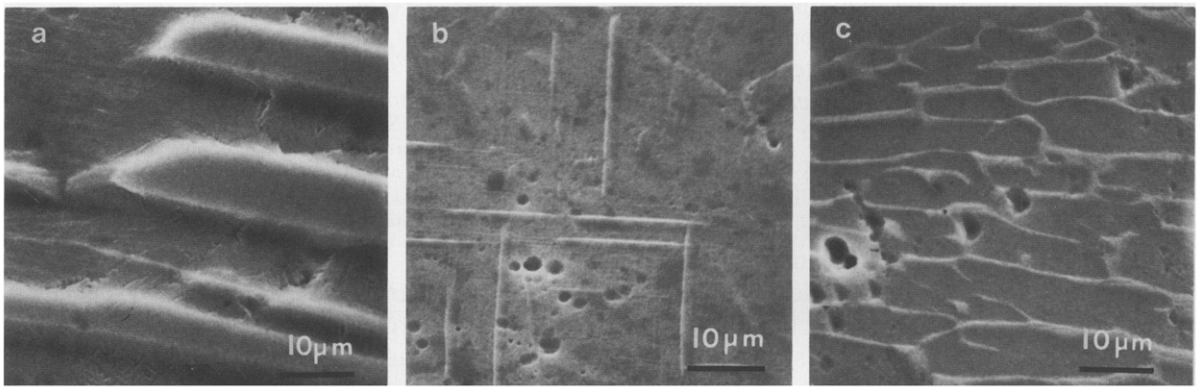

Fig. 4. SEM micrographs of etched cross-sections of the alloy after various STQ treatments. After STQ from 1200 and 1000 °C, the microstructure consists of α' martensite. After STQ from 800 °C, the microstructure consists of α phase and 10–20 vol.% of metastable $\beta + \alpha''$ phase. The pores are enlarged by etching.

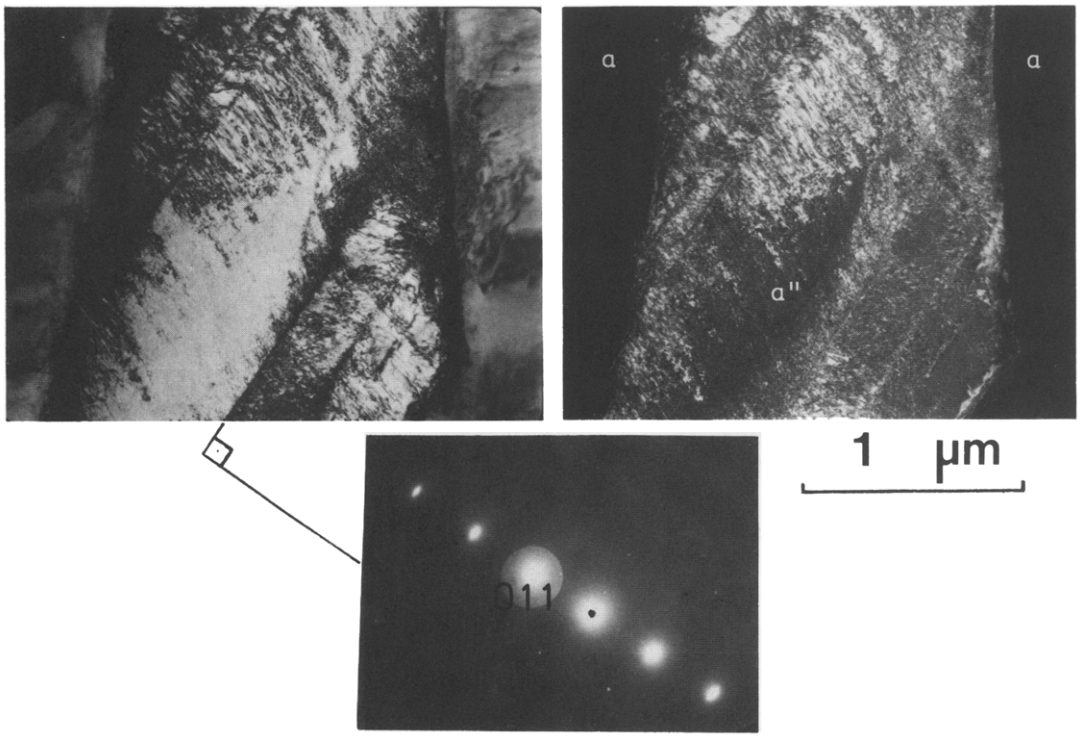

Fig. 5. Bright field and dark field TEM micrographs of metastable $\beta + \alpha''$ phase embedded between α grains in an 800 °C STQ treated Ti-6Al-4V specimen. The sample was tensile deformed at room temperature to 0.2% plastic strain. Twin laths in the β-α'' phase are along (011) planes of the metastable β phase. They contain fine dislocation-like internal defects, believed to be a form of strain-induced transformation to the orthorhombic α' martensite.

the smaller is the required stress for transformation. In this condition the alloy exhibits extreme softness and ductility. Figures 5 and 6 show stress-induced microstructural features in metastable β phase, obtained by quenching the alloy from 800 °C STQ, and subjecting it to subsequent tensile stress. The alloy samples were deformed in tension to 0.2% and 3% plastic strain respectively. The localized strains in the α'' phase regions are probably higher than that. The bright field image in Fig. 5 is full of dislocation-like or fine lath-like contrast which indicates twinning as a deformation mechanism. Duerig *et al.* [37] have described the mechanism of β to α'' transformation as one requiring simple atomic shuffles with a low activation barrier. The [100] diffraction pattern of Fig. 6 exhibits the cubic symmetry of the b.c.c. β lattice, but the diffraction spots are streaked and indicate the metastable character of the lattice. Figure 6 shows a shear band parallel to the (011) plane in this phase. This phase has an abnormally low Young's modulus (Section 3.3.1). As will be shown in Sections 3.3.2 and 3.3.3, the low Young's modulus is restored to higher values

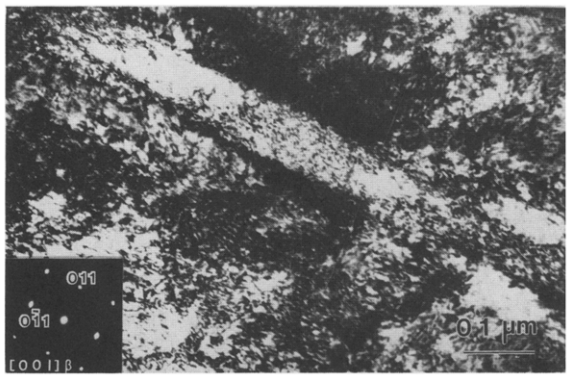

Fig. 6. TEM micrograph of the microstructure of metastable β phase in 800 °C STQ treated alloy after tensile deformation to 3% plastic strain. The diffraction spots in the [100] zone diffraction attern are streaked, a sign of the metastability of the lattice. A (011) shear band is visible in this highly distorted and dislocated phase.

by plastic deformation and by aging heat treatment. We interpret the strain-induced increase in Young's modulus as an indication of strain-induced phase transformation from metastable β to a more stable phase with higher modulus, *e.g.* the α'' phase.

3.2.3. Microstructures after aging

At a temperature of 200 °C thermal diffusion of interstitial and substitutional elements is negligible [14, 38]. Nevertheless, significant changes in modulus and damping occur at 200 °C (Section 3.3.3) which indicate that some microstructural rearrangement takes place in the metastable β or α'' phase. Internal stresses are believed to aid atomic rearrangement during aging. Aging treatment at a somewhat higher temperature, 350 °C, produces microstructural changes which can be directly observed by TEM. For example, fine tweed-like microstructure and twinning laths were observed in the β phase after aging for 1 h at 350 °C (Fig. 7(a)). The microstructure of metastable β phase was completely transformed after a 100 h aging treatment at 350 °C (Fig. 7(b)) to a mixture of stable vanadium-enriched β phase and α precipitates which approximately replicate the laths from the prior metastable β-α'' microstructure.

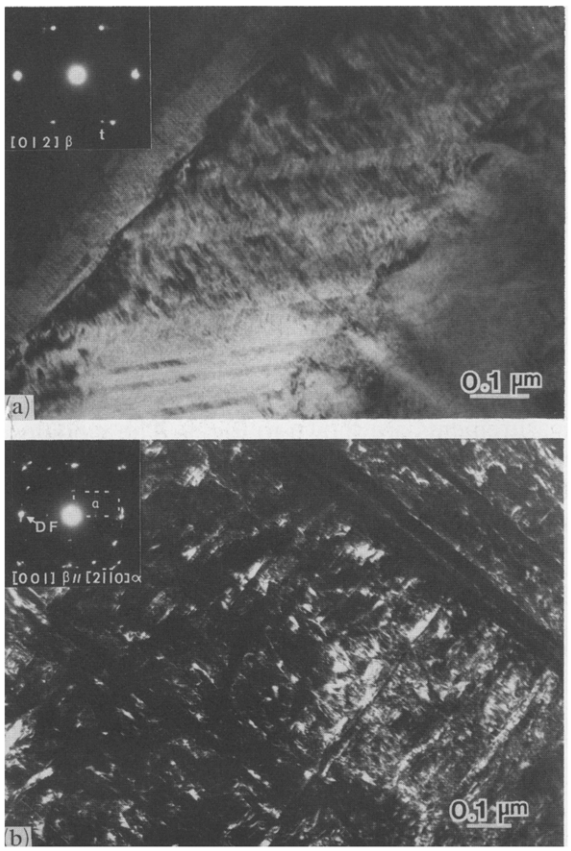

Fig. 7. TEM micrographs of the second phase in 800 °C STQ plus 350 °C aged alloy (a) after aging for 1 h and (b) after aging for 100 h. Internally faulted twin laths are seen in (a), similar to those in Fig. 5. The tweed-like background contrast is characteristic of phases going through a spinodal decomposition. In (b) the decomposition of the quenched metastable β phase has progressed to a fine mixture of stable β phase (probably enriched in vanadium to over 10 wt.%) and Burgers-oriented α precipitates.

3.3. Modulus and damping

3.3.1. Dependence of modulus and damping on solution treatment and quenching temperature

The results of longitudinal 66 kHz resonance vibration experiments on cylindrical specimens are shown in Fig. 8. They are room temperature data of samples which had been quenched from various solution treatment temperatures. The temperature dependences of Young's modulus and damping, determined from resonance flexural experiments, have been reported previously [17, 18, 24, 25], and a summary of their main findings is briefly reported here. Young's modulus decreases linearly in the temperature range from 300 to 700 K with a temperature coefficient of -0.049 GPa K^{-1} [25]. A large damping peak occurs at 140 K. At and above room temperature there exists a damping plateau with a relatively low damping coefficient of the order of 10^{-5}. This low damping capacity is typical of the relatively stable $\alpha+\beta$ phase mixtures of the Ti-6Al-4V alloy produced in manufacturing practices, such as after slow cooling from mill processing or heat treatment temperature. However, the damping capacity can be increased by

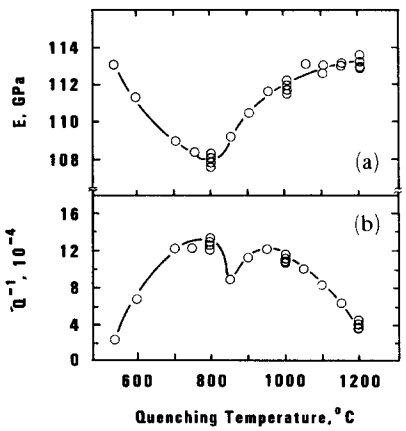

Fig. 8. (a) Young's modulus of Ti-6Al-4V alloy with 0.24 wt.% O *vs.* the temperature of STQ treatment. The minimum at 800 °C STQ corresponds to the presence of about 12 vol.% of metastable β-α'' phase mixture. (b) The room temperature damping capacity of the alloy is at a maximum after 800 °C STQ treatment. It corresponds to a transition state of the second phase between metastable β and α''. A second maximum at 950 °C STQ corresponds to the second phase's being in the transition of α'' to α'.

more than an order of magnitude when a metastable structure of the β phase is produced by quenching from solution heat treatment temperatures. Figure 8(b) shows two damping maxima at STQ temperatures of 800 and 950 °C.

An interpretation of the damping maxima is as follows. Tension–compression oscillation causes structural reversal of metastable phase conditions in an anelastic way, thus dissipating elastic strain energy. The 10 wt.% vanadium-enriched metastable β–α'' phase mixture has the largest specific damping capacity. It imparts a damping capacity $Q^{-1} = 12 \times 10^{-4}$ to the alloy, even though the volume fraction of the metastable phase is only 12% in this case. The lowest value of Young's modulus also occurs after STQ from 800 °C and is due to the same metastable β–α'' phase. It is well documented that the elastic constants of titanium alloys go through a minimum [15] at an electron per atom ratio of 4.1, which in the present case corresponds to 10 at.% or approximately 10 wt.% V alloy content.

The damping and the modulus values are mass-weighted averages of the contributions by the primary α phase and the second β, α'' or α' phase. The mass fractions can be approximated by the volume fractions f_a and f_b of α phase and the second phases respectively. The mass-weighted properties of the alloy are

$$Q_{\text{alloy}}^{-1} = f_a Q_a^{-1} + (1 - f_a) Q_b^{-1} \tag{8}$$

$$E_{\text{alloy}} = f_a E_a + (1 - f_a) E_b \quad \text{for phases in parallel} \tag{9a}$$

$$E_{\text{alloy}}^{-1} = f_a E_a^{-1} + (1 - f_a) E_b^{-1} \quad \text{for phases in series} \tag{9b}$$

where f_a is the volume fraction of α phase, and $1 - f_a$ is the volume fraction of the second phase. Because of the presence of a small amount of porosity (order of 0.5%), the sum $f_a + f_b$ is slightly less than unity. This error is neglected for the estimations of eqns. (8) and (9). The subscripts a and b refer to α phase and to the second (beta or martensite) phase respectively. On the basis of the structure evaluations in Section 3.2 and in ref. 27, α phase is essentially unchanged by STQ treatments. Therefore the specific damping and modulus values of the α phase may be taken as constants. For example, for the alloy with 0.24 wt.% O, $Q_a^{-1} \approx 5 \times 10^{-5}$ and $E_a \approx 113.5$ GPa. The specific values of the second phase are determined from eqns. (8) and (9) with the data in Fig. 8. Thus the specific damping capacity of the metastable 800 °C STQ β–α'' phase mixture is calculated as approximately 1×10^{-2}, while the Young's modulus of this phase is calculated by eqns. (9a) and (9b) as 68 GPa and 80 ± 7 GPa respectively, or an average of 74 GPa. This value is in good agreement with the Young's modulus value of 70 GPa of Ti–10wt.V alloy [15, 39, 40] whose composition is close to that of the second phase of 800 °C STQ Ti–6Al–4V. This agreement supports the assumption made above. It also supports the notion that modulus and damping variations of the Ti–6Al–4V alloy are entirely due to the structural changes in the second phase (β, α'' and α').

3.3.2. Modulus dependence on strain

Plastic deformation of a stable crystalline phase usually causes a negligibly small modulus change. Metastable phases, however, can undergo strain-induced phase transformation and as a consequence experience a significant modulus change. The change is proportional to the difference between the specific moduli of parent and product phases and to the volume fraction that actually undergoes the transformation. It was suspected that this phenomenon occurs in the soft metastable β–α'' phase of 800 °C STQ Ti–6Al–4V alloy. To verify this, 800 °C STQ alloy specimens were plastically strained, some in tension and others by transverse compression in a rolling mill, and were then evaluated by the resonant bar method. The results of Young's modulus measurements are shown in Fig. 9. The modulus increases linearly with strain, indicating that a soft phase is transformed into a stiffer phase, *e.g.* metastable quenched β phase is progressively transformed into α'' phase. The different slopes $dE/d\varepsilon$ of the two curves in Fig. 9 indicate that compressive deformation by rolling is more effective than tensile deformation in causing this phase transformation.

3.3.3. Dependence of modulus and damping in aging treatments

The softest (quenched) starting conditions permit the largest age-hardening effects. The aging responses are presented in Fig. 10 for one alloy containing 0.24 wt.% O for three starting conditions (800 °C STQ, 1000 °C STQ and 1200 °C STQ) and for three aging temperatures (200, 350 and 550 °C). The choice of the STQ condition determines the starting values of high damping and low modulus. The aging treatments

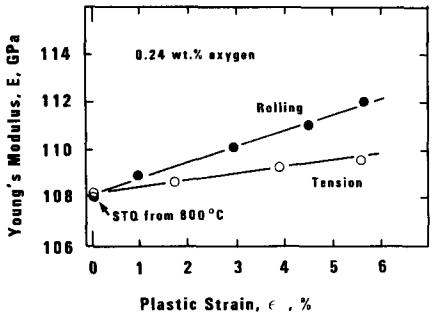

Fig. 9. Young's modulus of the 800 °C STQ treated alloy increases with plastic deformation. Compressive (rolling) strain is more effective than tensile strain. At the same time the damping capacity is reduced (not shown).

cause a rapid decrease in the damping capacity, whereas Young's modulus E recovers from low to higher values with aging time t. The magnitude of the modulus recovery rate dE/dt depends on the STQ starting condition and on the aging temperature. The greater the metastability of the quenched-in second phase and the higher the aging temperature, the faster is the recovery. Changes in damping and Young's modulus occur at aging temperatures as low as 200 °C, well below the temperature where interstitial or substitutional elements can diffuse in α- or β-Ti by thermal activation [14, 38]. Transformation of the metastable second phase is aided by thermal activation and by internal stress.

3.3.4. Dependence of Young's modulus and damping on oxygen concentration

Figure 11 shows the dependences for specimens of three different oxygen concentrations but of otherwise identical composition. The curves show the combined effects of oxygen concentration and aging heat treatment. The damping capacity decreases rapidly on aging, but it is insensitive to oxygen concentration (Fig. 11(b)). However, oxygen significantly increases Young's modulus. This increase is independent of the modulus increase caused by aging (Fig. 11(a)). Similar behavior was also found for other heat treatment conditions. For example, the plots of Young's modulus of the alloy with 0.24 wt.% O in Fig. 10 can be made into families of curves for other oxygen concentrations. A curve for a particular oxygen concentration may be obtained by shifting the curves by an amount ΔE, where ΔE is chosen in proportion to the oxygen

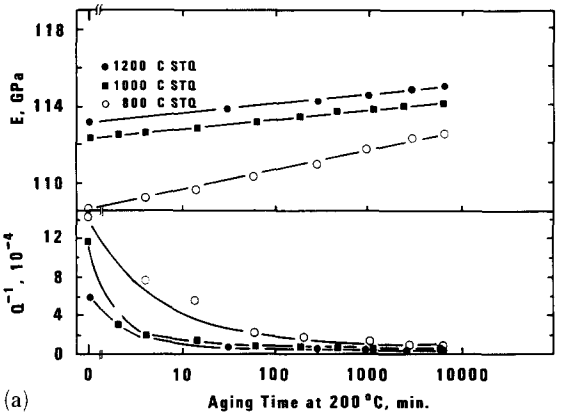

(a)

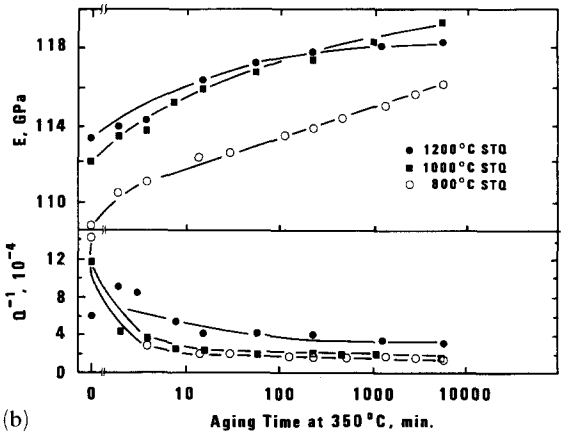

(b)

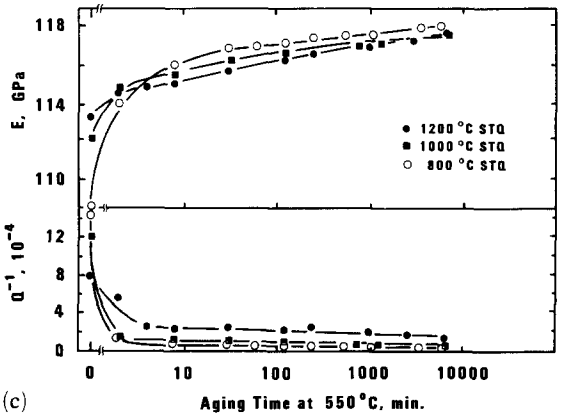

(c)

Fig. 10. Young's modulus and damping capacity at room temperature as a function of aging temperature and time: (a) aging at 200 °C, (b) aging at 350 °C, and (c) aging at 550 °C. In all cases the 800, 1000 and 1200 °C STQ treated alloys with their characteristic low Young's moduli and high damping capacities, *cf.* Fig. 8, served as the starting conditions. All aging treatments result in increased Young's modulus and decreased damping. All specimens contain 0.24 wt.% O.

concentration. Figure 12 shows the proportionality with oxygen concentration. The dependence of Young's modulus on both heat treatment and oxygen concentration may be written in the form

$$E_{alloy} = E_0(HT) + C_{ox}[O] \quad (10)$$

where $E_0(HT)$ is the Young's modulus of an oxygen-free alloy which is varied only by heat treatment (HT). C_{ox} is the oxygen coefficient of Young's modulus, and [O] is the concentration of dissolved oxygen.

The description in eqn. (10) may be expanded by adding an additional term to account for crystallographic orientation in a textured material, but such a term is zero for the present texture-free material. The plots of Young's modulus *vs.* oxygen concentration in Fig. 12 can be fitted by eqn. (10). The fitted parameter values are listed in Table 2 for the various heat treatments. The oxygen coefficients C_{ox} are in good agreement with each other (average value, 13.5 ± 0.5 GPa (wt.% O)$^{-1}$) for the specimens that started from a common STQ treatment, namely 800 °C STQ. The coefficient value for the 1000 °C STQ condition does not fit as well. Indeed, eqn. (10) is only approximately valid because its terms are not entirely independent of each other. Because oxygen increases the α:β phase volume ratio (see Fig. 3(a)) an indirect oxygen effect on $E_0(HT)$ is expected because α and β phases are affected in different ways by heat treatment. To illustrate this further, consider a combination of eqns. (9) and (10):

$$E_{alloy} = \underbrace{f_a E_a(HT)}_{1} + \underbrace{(1-f_a)E_b(HT)}_{2} + \underbrace{f_a C_{ox,a}[O]_a}_{3} + \underbrace{(1-f_a)C_{ox,b}[O]_b}_{4} \quad (11)$$

The meanings of the terms in this equation are analogous to those in eqns. (9) and (10). The first two right-hand terms represent roughly the heat-treatment-affected Young's modulus of oxygen-

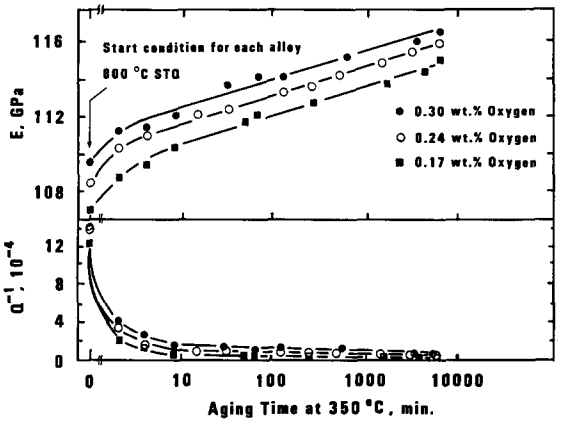

Fig. 11. The oxygen dependence of Young's modulus and room temperature damping capacity is shown for alloys of 0.17, 0.24 and 0.30 wt.% O. Heat treatments were identical for each alloy, namely 800 °C STQ followed by aging at 350 °C. It should be noted that the modulus differential is unchanged by aging treatments. Similar observations were made for other heat treatments. The effect of oxygen on damping is insignificant.

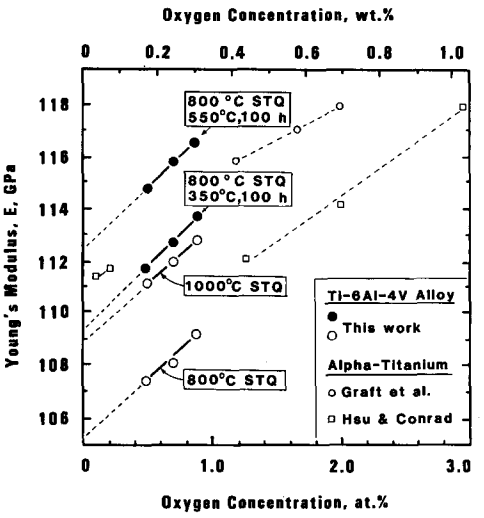

Fig. 12. The dependence of Young's modulus of Ti-6Al-4V alloy is shown as a function of oxygen concentration and heat treatments. The oxygen dependences of unalloyed α-Ti [5, 6] are shown for comparison.

TABLE 2 Values of E_0(HT) and C_{ox} in eqn. (10), derived from data in Fig. 12

Heat treatment	E_0(HT) (GPa)	C_{ox} (GPa (wt.% O)$^{-1}$)
800 °C STQ	105.2 ± 0.5	13.0
800 °C STQ + aging for 100 h at 300 °C	109.4 ± 0.5	14.0 } average, 13.5 ± 0.5
800 °C STQ + aging for 100 h at 550 °C	112.5 ± 0.5	13.5
1000 °C STQ	109.0 ± 0.5	9.4

TABLE 3 Effects of heat treatment and oxygen concentration on the parameters in eqn. (11)

Affected parameter	*Heat treatment effect*	*[O] effect*
f_a	Yes, particularly near transus temperature.	Yes, particularly near transus temperature.
$E_a(HT)$	No. Structure and bonding in α phase do not change.	No. E_a is the modulus of oxygen-free α phase.
$E_b(HT)$	Yes. Phase changes occur in metastable second phase.	No. E_b is the modulus of oxygen-free second phase.
$C_{ox,a}$	No. Same reason as for E_a.	No. Linear dependence on [O].
$C_{ox,b}$	Unknown. Present data do not permit evaluation because of dominance of α volume fraction.	Unknown. Present data do not permit evaluation because of dominance of α volume fraction.
$[O]_a/[O]_b$	Unknown. The partitioning of oxygen between different phases is unexplored.	Unknown. The partitioning of oxygen between different phases is unexplored.

free alloy, and the last two terms represent roughly the oxygen effect that is independent of heat treatment.

An inspection of the parameters (Table 3) indicates that the simple formula of eqn. (10) gives a good description if f_a does not change much with oxygen concentration. Such is the case for STQ heat treatments well below the transus temperature, *e.g.* 200 °C or more below the transus, but not for STQ treatments close to the transus, such as 1000 °C STQ. Some of the parameters' dependences cannot be evaluated from the present data. For example, it is believed that oxygen partitions preferentially into the α phase in a two-phase alloy. Partitioning would probably depend on heat treatment, but this is unexplored. Values of the oxygen coefficient $C_{ox,b}$ in the second phase cannot be extracted from the present data because the large volume fractions of α phase dominate the data. Experiments on samples that consist entirely of the second phase (β or α'') would be desirable. Despite the lack of the knowledge of the phase-specific parameters, eqn. (10) provides a useful and simple description of how Young's modulus depends on oxygen concentration and heat treatment.

A result worth emphasizing is the large increase in modulus caused by oxygen atoms. 1 at.% O increases Young's modulus by 4.5%, a 4–5-fold increase in bond stiffness per oxygen atom.

4. Conclusions

Young's modulus and damping capacity of Ti-6Al-4V are influenced by heat treatment. Quenching from certain solution treatment temperatures causes Young's modulus to be low. Aging heat treatments restore high modulus values. The contributions from two phases are considered: (1) from hexagonal α phase whose structure and composition varies little with heat treatment, and (2) from the second phase (α', α'' or β) whose structure and composition vary much with heat treatment. The specific modulus and the specific damping of the α phase can be taken as invariant with heat treatment. The major variables are the volume fractions of α and second phase and the specific modulus and damping capacity of the second phase. The largest changes in the phase volume fractions occur at and just below the transus temperature. The largest effects on modulus and damping are obtained in the second phase after quenching from around 800 °C. The specific property changes of the second phase (low modulus and high damping) are of such magnitude that a relatively small volume fraction of 10%–20% causes significant changes in the modulus and damping capacity of the alloy.

Oxygen increases Young's modulus with a linear concentration dependence. Its effect is approximately independent of heat treatment. The oxygen effect is additive to the modulus change from heat treatment. The room temperature damping capacity was, however, not significantly affected by oxygen.

Since texture was excluded in this study, isotropic values of Young's modulus and damping were obtained. The modulus values can be varied by as much as 10% and the damping capacity can be varied by more than an order of magnitude by choice of heat treatment and oxygen concentration. The individual effects are listed below.

4.1. Effect of solution treatment and quenching on Young's modulus

The lowest modulus value is obtained after STQ from around 800 °C. It is a weighted average of the specific modulus of the α phase and of the second phase of metastable β and α''. The modulus of α phase is essentially constant. The decreased modulus of the alloy is due to a soft metastable $\beta + \alpha''$ second phase. For example, the Ti-6Al-4V alloy with 0.24 wt.% O contains 88 vol.% α phase and 12 vol.% $\beta + \alpha''$ second phase (see Fig. 3). The phase-specific moduli are $E_\alpha \approx 113.5$ GPa and $E_{\beta+\alpha''} \approx 74$ GPa. Quenching from above the transus temperature produces all α' phase which is crystallographically isomorphous with α. Its modulus is approximately the same as that of the α phase. Nevertheless, aging heat treatments increase the modulus somewhat, indicating that the α' phase contains some metastable phase constituent in the quenched state.

4.2. Effect of aging heat treatments on Young's modulus

In all cases the modulus is increased by aging. The largest increase is obtained when starting with the softest STQ condition. Even at the low aging temperature of 200 °C, at which thermal diffusion of alloy elements cannot take place, significant modulus increases are obtained. A speculative explanation is that distortions in the quenched α' and α'' structures lower the activation barrier for transformation and enable atomic rearrangement in the highly strained regions, such as in the interface regions of α' and α'' martensite laths or at the boundaries between metastable β phase and α'' phase.

4.3. Effect of plastic deformation on Young's modulus

Plastic deformation causes transformation of metastable β into α'' martensite phase. It is similar to that achieved by aging, and it causes an increase in Young's modulus. On the basis of the data in Fig. 9, and assuming that the modulus increase is entirely due to transformation within the soft (metastable $\beta + \alpha''$) phase, a rolling strain of 5.5% causes the specific modulus of the soft phase to increase from about 74 GPa to over 100 GPa. The same strain in tension causes only half as much modulus increase. A volume decrease associated with the transformation of metastable β into α'' would explain the different responses to tension and compression.

4.4. Effect of oxygen concentration on Young's modulus

A linear increase in modulus with oxygen concentration was found for several heat-treated conditions. The proportionality coefficient C_{ox} listed in Table 2 is approximately independent of heat treatment and of the phases present.

4.5. Effect of heat treatment on damping Q^{-1}

The damping capacity of furnace-cooled or of aged Ti-6Al-4V alloy is generally quite small, *i.e.* less than 1×10^{-4}. STQ conditions have higher damping capacities. The highest values ($Q^{-1} = 13 \times 10^{-4}$) occur after STQ from 800 °C. The damping is caused by the same metastable ($\beta + \alpha''$) phase that causes the minimum in Young's modulus. The specific damping capacity of this metastable phase mixture is of the order of 10^{-2}.

A second maximum in the room temperature damping capacity ($Q^{-1} = 12 \times 10^{-4}$) occurs after STQ from 950 °C. In this condition the alloy contains approximately 50 vol.% of second phase, which is in the transition state between hexagonal α' and orthorhombic α'' structures. The other 50 vol.% of the microstructure consists of primary α phase, which has a low specific damping capacity (less than 1×10^{-4}) at room temperature.

Aging causes a rapid decrease in damping capacity. It permits transformation of the metastable phases (metastable β or α'' or α') into phase mixtures of higher stability. At a relatively high aging temperature, *e.g.* 550 °C, at which diffusion of the alloy elements occurs readily, the metastable phases transform completely into α phase and stabilized vanadium-rich β phase (more than about 15 wt.% V). Low overall damping capacity is the consequence.

4.6. Effect of oxygen on the damping capacity

In the concentration range up to 0.30 wt.%, oxygen had a negligible effect on the room temperature damping capacity.

Acknowledgments

Dr. David Ro, who was with Imperial Clevite Corporation, Cleveland, OH, provided the sintered Ti-6Al-4V specimens with the various oxygen concentrations. One of us, Y. T. Lee, is

grateful to Dr. J. Talia for instruction in the experimental procedures for the resonance vibration experiments. The work was supported by the National Science Foundation under Grant DMR 81-21772.

References

1 P. E. Armstrong and H. L. Brown, *Trans. Metall. Soc. AIME, 230* (1964) 962–966.
2 F. Larson and A. Zarkades, *Battelle Columbus Laboratories Rep. MCIC-74-20*, 1974, pp. 1–76.
3 A. Zarkades and R. F. Larson, Elasticity of titanium sheet alloys. In R. I. Jaffee and N. E. Promisal (eds.), *The Science, Technology and Application of Titanium*, Pergamon, Oxford, 1970, pp. 933–941.
4 E. S. Fisher and G. J. Renken, *Phys. Rev., 135* (2A) (1964) A482.
5 W. H. Graft, D. W. Levinson and W. Rostoker, *Trans. Am. Soc. Met., 49* (1957) 263–279.
6 N. Hsu and H. Conrad, *Scr. Metall., 5* (1971) 905–908.
7 H. Conrad, Effect of interstitial solutes on the strength and ductility of titanium. In J. W. Christian, P. Haasen and T. B. Massalski (eds.), *Progress in Materials Science*, Vol. 26, Pergamon, Oxford, 1981, p. 136.
8 G. Welsch and W. Bunk, *Metall. Trans. A, 13* (1982) 889–899.
9 A. W. Bowen and C. A. Stubbington, *Titanium and Titanium Alloys, Scientific and Technological Aspects*, Vol. 3, Plenum, New York, 1982, pp. 1989–2001.
10 Y. T. Lee, K.-J. Grundhoff and G. Wirth, *Z. Metallkd., 78* (1987) 49–57.
11 G. W. Yoder, L. A. Cooley and T. W. Crooker, *Metall. Trans. A, 8* (1977) 1737–1743.
12 P. J. Fopiano, M. B. Bever and B. L. Averbach, *Trans. Am. Soc. Met., 62* (1969) 324–332.
13 E. A. Brandes (ed.), *Smithells Metals Reference Book*, Butterworths, London, 1982, 6th edn., Chap. 15.
14 U. Zwicker, *Titan und Titanlegierungen*, Springer, Berlin, 1974.
15 E. W. Collings, *Physical Metallurgy of Titanium Alloys*, American Society for Metals, Metals Park, OH, 1984.
16 D. W. James, *Mater. Sci. Eng., 18* (1969) 1–8.
17 Y. T. Lee and G. Welsch, in G. Lütjering, U. Zwicker and W. Bunk (eds.), *Titanium Science Technology, Proc. 5th Int. Conf. on Titanium, 1984*, Deutsche Gesellschaft für Metallkunde, Oberursel, 1985, pp. 1689–1696.
18 Y. Ito, Y. Moriguchi, N. Nagai, A. Hiromoto, Y. Takedo, T. Daikoku and S. Ueda, in H. Kimura and O. Izumi (eds.), *Titanium '80 Science and Technology, Proc. 4th Int. Conf. on Titanium, 1980*, Metallurgical Society of AIME, Warrendale, PA, 1980, pp. 593–600.
19 K. Sugimoto, K. Kamei, T. Sugimoto, Y. Nakamura, K. Nakao and M. Nishida, in P. Lacombe, R. Tricot and G. Beranger (eds.), *Proc. 6th World Conf. on Titanium, Cannes, 1988*, Les Editions de Physique, Les Ulis, 1989, pp. 81–86.
20 Y. Ito *et al.*, in G. Lutjering, U. Zwicker and W. Bunk (eds.), *Titanium Science and Technology, Proc. 5th Int. Conf. on Titanium, 1984*, Deutsche Gesellschaft für Metallkunde, Oberursel, 1985, pp. 1643–1650, 1683–1688.
21 Y. Ito *et al.*, in H. Kimura and O. Izumi (eds.), *Titanium '80, Proc. 4th Int. Conf. on Titanium, 1980*, Metallurgical Society of AIME, Warrendale, PA, 1980, pp. 593–600.
22 E. Török and J. P. Simpson, in H. Kimura and O. Izumi (eds.), *Titanium '80, Proc. 4th Int. Conf. on Titanium, 1980*, Metallurgical Society of AIME, Warrendale, PA, 1980, pp. 601–610.
23 J. P. Simpson and E. Török, in H. Kimura and O. Izumi (eds.), *Titanium '80, Proc. 4th Int. Conf. on Titanium, 1980*, Metallurgical Society of AIME, Warrendale, PA, 1980, pp. 611–620.
24 G. Welsch and M. Weller, Damping of Ti–6Al–4V. In B. B. Rath and M. S. Misra (eds.), *Role of Interfaces on Materials Damping*, American Society for Metals, Metals Park, OH, 1985, pp. 73–78.
25 M. Weller, Y. T. Lee and G. Welsch, unpublished results, MPI Stuttgart, 1984.
26 A. I. Kahveci and G. Welsch, *Scr. Metall., 20* (1986) 1287–1290.
27 Z. Liu and G. Welsch, *Metall. Trans. A, 19* (1988) 527–542.
28 ASTM B328-73, *Annual Book of ASTM Standards*, Part 9, ASTM, Philadelphia, PA, 1980.
29 G. Welsch, Y. T. Lee, P. C. Eloff, D. Eylon and F. H. Froes, *Metall. Trans. A, 14* (1983) 761–769.
30 Y. T. Lee, M. Peters and G. Wirth, *Mater. Sci. Eng., A102* (1988) 105–114.
31 K. M. Entwistle, in B. Chalmers and A. G. Quarrel (eds.), *Physical Examination of Metals*, Edward Arnold, London, 1960, pp. 487–550.
32 T. A. Read, *Phys. Rev., 58* (1940) 371.
33 J. Marx, *Rev. Sci. Instrum., 22* (7) (1951) 503–509.
34 R. Castro and L. Seraphin, *Mem. Sci. Rev. Metall., 63* (1966) 1025–1058.
35 A. Lasalmonie and M. Loubradou, *J. Mater. Sci., 14* (1979) 2589–2595.
36 M. Peters, *Metallurgia, 37* (6) (1983) 584–589.
37 T. W. Duerig, R. M. Middleton, G. T. Terlinde and J. C. Williams, in *Titanium '80 Science and Technology, Proc. 4th Int. Conf. on Titanium*, Vol. 2, Metallurgical Society of AIME, Warrendale, PA, 1980, pp. 1503–1512.
38 Z. Liu and G. Welsch, *Metall. Trans. A, 19* (1988) 1121–1124.
39 S. G. Fedotov, *Titanium and its Alloys*, Israel Programme for Scientific Translations, Israel, Publ. No. 10, 1966, p. 199 (I. I. Kornilov (ed.)).
40 S. G. Fedotov, in R. I. Jaffee and H. M. Burte (eds.), *Titanium Science and Technology*, Plenum, New York, 1973, pp. 871–881.